

Kardar-Parisi-Zhang Physics in the Density Fluctuations of Localized Two-Dimensional Wave Packets

Sen Mu,^{1,*} Jiangbin Gong,^{1,2,3,4,†} and Gabriel Lemarié^{1,2,3,5,‡}


¹*Department of Physics, National University of Singapore, Singapore 117542, Singapore*

²*Centre for Quantum Technologies, National University of Singapore, Singapore 117543, Singapore*

³*MajuLab, CNRS-UCA-SU-NUS-NTU International Joint Research Unit, Singapore*

⁴*Joint School of National University of Singapore and Tianjin University, International Campus of Tianjin University, Binhai New City, Fuzhou 350207, China*

⁵*Laboratoire de Physique Théorique, Université de Toulouse, CNRS, UPS, France*

 (Received 14 June 2023; revised 8 September 2023; accepted 14 December 2023; published 23 January 2024)

We identify the key features of Kardar-Parisi-Zhang (KPZ) universality class in the fluctuations of the wave density logarithm in a two-dimensional Anderson localized wave packet. In our numerical analysis, the fluctuations are found to exhibit an algebraic scaling with distance characterized by an exponent of $1/3$, and a Tracy-Widom probability distribution of the fluctuations. Additionally, within a directed polymer picture of KPZ physics, we identify the dominant contribution of a directed path to the wave packet density and find that its transverse fluctuations are characterized by a roughness exponent $2/3$. Leveraging on this connection with KPZ physics, we verify that an Anderson localized wave packet in 2D exhibits a stretched exponential correction to its well-known exponential localization.

DOI: [10.1103/PhysRevLett.132.046301](https://doi.org/10.1103/PhysRevLett.132.046301)

Introduction.—Universality of fluctuations, a remarkable phenomenon pervading physics, is exemplified by the central limit theorem, which characterizes the convergence to a normal distribution for the sum of independent random variables, and describes for instance the behavior of particles in Brownian motion [1–3]. Another example is the Kardar-Parisi-Zhang (KPZ) physics, a universal framework that is relevant to diverse processes ranging from interface growth to directed polymers [4–8]. While initially associated with classical systems, recent numerical and experimental investigations have revealed KPZ physics in quantum systems, including one-dimensional quantum magnets [9–11], random unitary circuits [12], and driven-dissipative quantum fluids [13].

Anderson localization is a phenomenon where the wave function of a particle becomes localized due to disorder, hindering its diffusion [14–16]. Universal fluctuations play a key role in different aspects of this phenomenon, including universal conductance fluctuations [17,18], random matrix statistics [19], log-normal distributions in one-dimensional localized systems [20] and multifractal statistics in the critical regime of the Anderson transition [21–25] of diverse observables.

While one-dimensional Anderson localization is exactly solvable [19,22,26–29], understanding higher-dimensional cases and fluctuations in the localized regime remains a challenge. Theoretically, one can start from the regime of strong disorder and high dimensions and use the forward scattering approximation, which suggests an analogy with directed polymers [30–36]. However, this approximation is

uncontrolled beyond the regime of strong disorder and predicts a transition even in dimensions one and two, contradicting established properties. Numerical simulations in two dimensions reveal an analogy with KPZ physics for a specific observable, namely, the conductance at zero temperature. It exhibits fluctuations belonging to the KPZ universality class [37–40] and displays glassy properties akin to directed polymers [41]. However, electron transport in the localized regime is influenced by temperature and interactions, leading to observations of electron glass physics rather than KPZ physics in experiments [42–51].

Recent experimental studies on Anderson localization utilizing cold atoms, light waves, and ultrasounds [52–62] have shed light on another type of transport, namely the expansion of a wave packet. This fresh perspective offers an *in situ* and dynamical depiction of localization that differs from the conductance. Furthermore, localization in these platforms can be finely controlled, allowing for examination of a regime in which interaction and temperature effects are negligible. For example, cold atoms have provided an experimental confirmation of a three-dimensional Anderson metal-insulator transition, with a critical exponent that aligns with numerical predictions [63,64]. We are thus motivated to study the universality of directly measurable fluctuations in the spatial profile of wave packets in Anderson localized systems. This problem is distinctly separate from conductance fluctuations, as evidenced by extensive research focused on wave packets. Importantly, our Letter establishes a clear and strong connection between fluctuations of spatial profile of wave packets with KPZ physics.

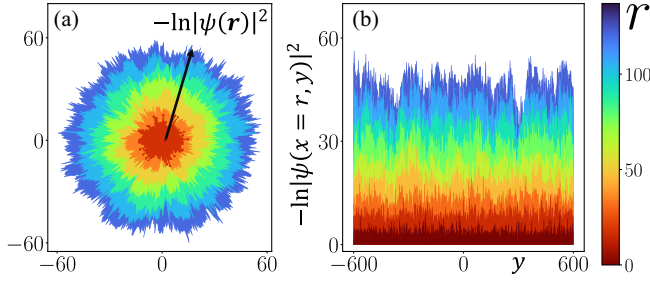


FIG. 1. The logarithm of the wave density $\ln|\psi(\mathbf{r})|^2$ of a 2D localized wave packet exhibits similar growth with distance r as a rough surface in the Kardar-Parisi-Zhang universality class [65]. We present the results of long-time evolution for two different initial conditions: (a) a “circular” peak at $\mathbf{0}$, Eq. (2), and (b) a “flat” line along y at $x = 0$, Eq. (3). We plot the transformed coordinates $[-\ln|\psi(\mathbf{r})|^2(x/r), -\ln|\psi(\mathbf{r})|^2(y/r)]$ in (a) and $(y, -\ln|\psi(x=r, y)|^2)$ in (b), with different colors representing various distances r . Numerical simulations were conducted using model Eq. (1), a variant of the kicked rotor, with system size 600×600 , kick strength $K = 1.21$, coupling $\epsilon = 0.1$, and evolution time $t = 10^4$.

We examine the fluctuations of the wave density of an exponentially localized wave packet in two dimensions. Using exact numerical simulations, we demonstrate that the fluctuations of the logarithm of the wave density correspond to the height of a rough surface in the KPZ universality class [65]; see Fig. 1. We find that these fluctuations scale algebraically with distance, with a fluctuation exponent of $1/3$, and identify the dominant contributing paths and their transverse fluctuations characterized by a roughness exponent of $2/3$. Moreover, we demonstrate that the distribution of the logarithm of the wave density follows the Tracy-Widom distribution. These findings firmly establish that two-dimensional localized wave packets belong to the KPZ universality class. Leveraging the well-established analytical knowledge of KPZ physics [7,66–70] offers valuable new perspectives on the intricate characteristics of Anderson localization in two dimensions. It not only sheds light on the underlying mechanisms but also reveals intriguing features, such as the presence of a stretched exponential correction to the exponential behavior of localization in two dimensions.

Model.—In order to describe the unitary dynamics of a wave packet in a two-dimensional discrete square lattice, we have used a variant of the quantum kicked rotor [71–75] described by the following quantum map:

$$|\psi_{t+1}\rangle = \hat{U}|\psi_t\rangle = e^{-iKV(\hat{k})} e^{-iW(\hat{p})} |\psi_t\rangle. \quad (1)$$

This quantum map evolves the wave packet state $|\psi_t\rangle$ at time t to the state at time $t + 1$ by applying an evolution operator \hat{U} written as the product of an operator $e^{-iW(\hat{p})}$ of random on-site phases and a kick operator $e^{-iKV(\hat{k})}$ playing the role of hopping amplitudes in the Anderson model [72].

Here, $\mathbf{r} = (x, y)$ denotes site position on the discrete lattice and $\mathbf{k} = (k_x, k_y)$ with $k_x, k_y \in [-\pi, \pi)$, the wave vector reciprocal to the lattice: $\psi_t(\mathbf{k}) = \sum_{\mathbf{r}} \psi_t(\mathbf{r}) e^{-i\mathbf{k}\cdot\mathbf{r}}$. The random on-site phases $W(\mathbf{r})$ are independent, identically distributed uniformly in the interval $[-\pi, \pi]$, and the kick operator $e^{-iKV(\hat{k})}$ is parametrized by the kicking strength K and $V(\mathbf{k}) = \cos k_x + \cos k_y + \epsilon \cos k_x \cos k_y$ with ϵ a non-zero coupling parameter. The quantum kicked rotor has been instrumental in understanding phenomena such as Anderson localization and the Anderson transition, both theoretically and experimentally [52,53,62,63,71–77].

In this Letter, the initial condition of the wave packet plays an important role. We consider two types: peaked either at a particular site on the square lattice, Eq. (2), or a line on the lattice, Eq. (3). The two initial conditions are referred to as circular and flat initial conditions, respectively, in the context of KPZ physics [65]. More specifically, such two types of initial states are

$$\text{circular: } \psi_0(\mathbf{r}) = \delta(\mathbf{r}), \quad r \equiv \sqrt{x^2 + y^2}, \quad (2)$$

$$\text{flat: } \psi_0(x, k_y) = \delta(x)\delta(k_y), \quad r \equiv x, \quad (3)$$

where r represents the distance in the localization direction along which the wave packet decays exponentially from the initial condition.

Approximate mapping to a directed polymer problem.—The directed polymer (DP) problem in $(1 + 1)$ dimensions is a rare example of an analytically solvable model belonging to the KPZ universality class; see, e.g., [67,68,70]. We will employ the forward scattering approximation [30,31,33] to establish an approximate mapping from two-dimensional localized wave packets to a $(1 + 1)$ -dimensional DP model in the strong disorder regime, corresponding to a small kicking strength ($K \ll 1$) in Eq. (1). Starting with a circular initial condition, Eq. (2), we express the wave packet $\psi_t(\mathbf{r})$ using a path integral representation:

$$\psi_t(\mathbf{r}) = \langle \mathbf{r} | \hat{U}^t | \mathbf{0} \rangle = \sum_{\mathbf{r}_{t-1}} \dots \sum_{\mathbf{r}_1} \langle \mathbf{r} | \hat{U} | \mathbf{r}_{t-1} \rangle \dots \langle \mathbf{r}_1 | \hat{U} | \mathbf{0} \rangle. \quad (4)$$

When $K \ll 1$, hoppings are mainly limited to nearest neighbors with a small amplitude $|J_0| \ll 1$. Consequently, we can approximate the path integral for $\psi_t(\mathbf{r})$ by keeping only the shortest, directed paths denoted DP. In the limit of large times, we find (see SM [78])

$$\psi_t(\mathbf{r}) \approx J_0^r \sum_{\text{DP}} \prod_{\mathbf{r}_j \in \text{DP}} e^{-\tilde{W}(\mathbf{r}_j)} \quad (5)$$

In this equation, $\tilde{W}(\mathbf{r}_j)$ are complex numbers that have a direct relationship with $W(\mathbf{r}_j)$. The resulting expression resembles the partition function of a DP with a complex on-site disorder. In dimension two, numerical evidence shows that the scaling properties of such complex DP problem are

identical to those with real disorder [79–85], confirming their belonging to the KPZ universality class. In the following, we will refine our analysis beyond the previous uncontrolled approximation and beyond the strong disorder regime ($K \ll 1$), now employing exact numerical simulations (for $K \approx 1$) to conclusively establish the connection with the KPZ universality class.

Exponential localization as a rough surface growth.— Let us investigate the spatial properties of the wave density $|\psi_t(\mathbf{r})|^2$ after evolving our initial state, Eq. (2) or Eq. (3), for times $t \gg t_{\text{loc}}$ much larger than the localization time (see SM [78]), when the envelope of the wave packet is stationary. We will postpone the discussion on the effects of time and omit the label of time for the wave density in the following, i.e., $|\psi(\mathbf{r})|^2 \equiv |\psi_t(\mathbf{r})|^2$. Consider the logarithm of the wave density $\ln |\psi(\mathbf{r})|^2$ at a distance r from the initial location. The analogy that we have drawn in the previous section leads us to interpret $-\ln |\psi(\mathbf{r})|^2$ as the analog of the height function h of a growing rough surface (or, equivalently, as the free energy of a directed polymer problem), where the distance r along the localization direction in our model is understood as the time in the surface growth (or directed polymer) process. In Fig. 1, we present this effective growth for both circular, Eq. (2), and flat, Eq. (3), initial conditions. The striking resemblance between these plots and experimental observations in liquid crystal nematics [65] will be quantitatively validated in the following.

Given the KPZ physics analogy and insights from one-dimensional Anderson localization [20], we anticipate the logarithm of the wave packet density $|\psi(\mathbf{r})|^2$ to behave as follows [38,65,86,87]:

$$\ln |\psi(\mathbf{r})|^2 \underset{r \gg \xi}{\approx} -\frac{2r}{\xi} + \left(\frac{r}{\xi}\right)^\beta \Gamma \chi(\mathbf{r}) + \Lambda, \quad (6)$$

where χ is a random variable of order 1, Γ and Λ are constants. The first term corresponds to exponential localization, with ξ the localization length, while the second term captures fluctuations with a fluctuation growth exponent β . In two dimensions, β differs from the known value 1/2 for Anderson localization in one dimension [20]. Figure 2 shows the behavior of the standard deviation $\sigma[\ln |\psi(\mathbf{r})|^2]$ of $\ln |\psi(\mathbf{r})|^2$, which grows algebraically with r as $\sigma \sim r^\beta$. The fluctuation exponent $\beta \approx 1/3$, consistent with the KPZ universality class.

Optimal path and roughness exponent.—The optimal trajectory of a directed polymer in a random medium reveals important insights into the system’s dynamics and glassy properties [86,88,89]. By extending the approach in [41], we can visualize the optimal path associated with a wave packet localized in a specific disorder configuration. This is achieved by examining the response of the wave density at \mathbf{r} to a local perturbation of the disorder at \mathbf{r}' , where the perturbation involves shifting the on-site phase $W(\mathbf{r}')$ by π . We quantify this response using

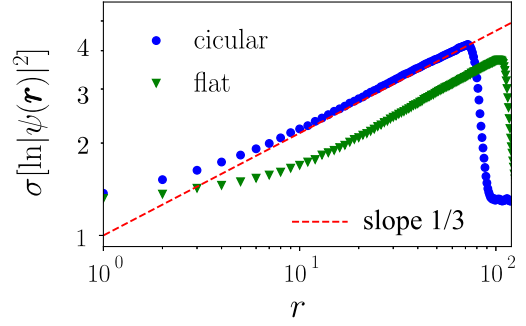


FIG. 2. We examine the scaling of fluctuations in $\ln |\psi(r)|^2$ with distance r from two initial conditions: (a) circular initial condition, Eq. (2), and (b) flat initial condition, Eq. (3). The standard deviation $\sigma[\ln |\psi(\mathbf{r})|^2]$ is plotted along the diagonal of the square lattice $x = y$ (with distance $r = \sqrt{x^2 + y^2}$) in (a), and along the line along x at $y = 0$ (with distance $r = x$) in (b). The dashed line represents the expected algebraic behavior $\sigma[\ln |\psi(\mathbf{r})|^2] \sim r^{1/3}$ based on the analogy with KPZ physics. Numerical simulations are performed on system Eq. (1) with size 300×300 , kick strength $K = 1.04$, coupling $\epsilon = 0.1$, and evolution time $t = 10^3$. For both initial conditions, 10^5 disorder realizations are considered.

$$\rho_r(\mathbf{r}') \equiv \frac{|\tilde{\psi}_{r'}(\mathbf{r})|^2 - |\psi(\mathbf{r})|^2}{|\psi(\mathbf{r})|^2}, \quad (7)$$

which measures the difference between the wave densities with or without perturbation ($|\tilde{\psi}_{r'}(\mathbf{r})|^2$ or $|\psi(\mathbf{r})|^2$, respectively). In the strongly localized regime ($r \gg \xi$), the response becomes highly inhomogeneous, concentrated along a specific path that depends on both the disorder configuration, initial condition, and final point \mathbf{r} . In Fig. 3(a), we illustrate such a path, where the red dot represents the final site \mathbf{r} , and the green line corresponds to the flat initial condition along the line $x = 0$ [Eq. (3)].

Let us delve deeper into the properties of the optimal path. Considering the same flat initial condition, we focus on the transverse position Y at $x = 0$ of the optimal path for the wave packet at $\mathbf{r} = (x, 0)$. The calculation of Y relies on the response ρ_r at $x' = 0$, given by

$$Y = \frac{\sum_{y'} y' \rho_r(0, y')}{\sum_{y'} \rho_r(0, y')}, \quad (8)$$

where $\rho_r(0, y') / \sum_{y'} \rho_r(0, y')$ represents the normalized probability distribution of the optimal trajectory. In the directed polymer problem, the optimal path arises from a global optimization over the disorder, resulting in a path that exhibits more wandering compared to a simple random walk. This wandering behavior is characterized by the roughness exponent ζ , which relates the standard deviation of the expected transverse position to the distance r from the initial condition [Eq. (3)]: $\sigma[Y] \sim r^\zeta$. Numerical results on the roughness exponent are presented in Fig. 3(b),

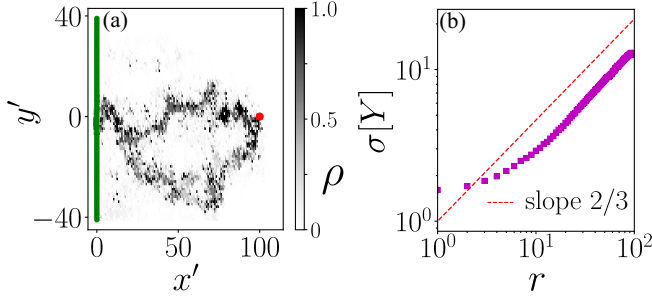


FIG. 3. (a) The optimal path for a wave packet originating from a flat initial condition, Eq. (3), represented by the green line along y at $x = 0$, propagates to the final site $\mathbf{r} = (x = 100, y = 0)$ shown as the red dot. The local response $\rho_r(\mathbf{r}')$, Eq. (7), is displayed as a color plot, with $\rho_r(\mathbf{r}') = 1$ if $\rho_r(\mathbf{r}') > 1$ for better visibility. (b) The scaling of the standard deviation $\sigma[Y]$ of the transverse position Y , Eq. (8), of the optimal path is shown as a function of the distance $r = x$ from the flat initial condition, Eq. (3). The dashed line represents the expected algebraic behavior $\sigma[Y] \sim r^{2/3}$ based on KPZ physics. The numerical simulations employ the model described by Eq. (1) with a system size of 300×300 , kick strength $K = 1.04$, coupling $\epsilon = 0.1$, evolution time $t = 10^3$, and an averaging over 10^4 disorder realizations.

clearly indicating $\zeta \approx 2/3$. This discovery shows differing wave packet fluctuations in the localization (time) and transverse (space within KPZ physics) directions. This asymmetry, a nontrivial signature of KPZ physics, arises from Anderson localization itself.

Tracy-Widom distribution and the shape of a 2D localized wave packet.—Drawing from the analogy with the DP problem, the random variable χ in Eq. (6) is expected to follow a universal distribution function. Specifically, for the circular initial condition, it should obey the Tracy-Widom (TW) distribution of the Gaussian unitary ensemble (GUE). In Fig. 4(a), we present the distribution of $\tilde{\chi}(\mathbf{r}) = (\ln |\psi(\mathbf{r})|^2 - \langle \ln |\psi(\mathbf{r})|^2 \rangle) / \sigma[\ln |\psi(\mathbf{r})|^2]$ alongside the GUE TW distribution $P_{\text{TW}}(\tilde{\chi})$, rescaled to have zero mean and unit standard deviation. We observe a good agreement between the two.

This makes it possible to determine the shape of a localized wave packet. The form of the typical wave density follows from an average of the result in Eq. (6):

$$\langle \ln |\psi(\mathbf{r})|^2 \rangle_{r \gg \xi} \approx -\frac{2r}{\xi} + \left(\frac{r}{\xi}\right)^{1/3} \Gamma\mu + \Lambda, \quad (9)$$

where $\langle \dots \rangle$ denotes disorder averaging at fixed r and $\mu \approx -1.77$ is the nonzero mean of the GUE TW distribution. Figure 4(b) shows a very good agreement between this prediction Eq. (9) and numerical data for $\langle \ln |\psi(\mathbf{r})|^2 \rangle$ at large $r \gg \xi$.

The average wave density $\langle |\psi(\mathbf{r})|^2 \rangle$ can be determined by considering the typical wave packet and the fluctuations around it, following the GUE TW distribution $P_{\text{TW}}(\tilde{\chi})$. This average wave packet profile is experimentally

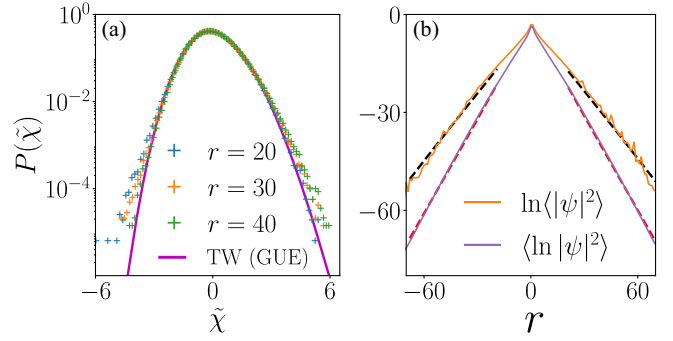


FIG. 4. Tracy-Widom distribution and the shape of a 2D localized wave packet. (a) The distribution of the rescaled wave density $\tilde{\chi}$, defined as $(\ln |\psi(\mathbf{r})|^2 - \langle \ln |\psi(\mathbf{r})|^2 \rangle) / \sigma[\ln |\psi(\mathbf{r})|^2]$, exhibits good agreement with the GUE Tracy-Widom distribution (magenta line) for the circular initial condition, Eq. (3). Crosses of different colors represent different distances r from the initial condition, and their collapse onto the Tracy-Widom distribution confirms the scaling behavior given by Eq. (6). (b) The typical wave density $\langle \ln |\psi(\mathbf{r})|^2 \rangle$ (lower violet line) and the logarithm of the average wave density $\ln \langle |\psi(\mathbf{r})|^2 \rangle$ (upper orange line) are displayed. The red dashed line represents a fit using Eq. (9) with $\xi \approx 1.7$, $\Gamma \approx -4.0$, and $\Lambda \approx -15.2$. The upper black dashed line represents Eq. (10) with $\Gamma' \approx 2.0$, $\Gamma'' \approx 2.4$, and $\Lambda' \approx -9.9$, determined from the typical wave density and the GUE Tracy-Widom distribution. Numerical data is obtained from the model described by Eq. (1), considering \mathbf{r} on the diagonal $x = y$ of a square lattice with size 300×300 . The simulations employ a kick strength of $K = 1.0$, coupling $\epsilon = 0.1$, an evolution time of $t = 10^3$, and involve 10^6 disorder realizations.

accessible, for instance, with cold atoms; see, e.g., [55,62,76]. After some algebraic manipulations (see SM [78] for details), we obtain the approximation

$$\begin{aligned} \langle |\psi(\mathbf{r})|^2 \rangle_{r \gg \xi} &\approx e^{\langle \ln |\psi(\mathbf{r})|^2 \rangle} \int_{-\infty}^{\infty} d\tilde{\chi} e^{\tilde{\chi} \sigma[\ln |\psi(\mathbf{r})|^2]} P_{\text{TW}}(\tilde{\chi}) \\ &\approx e^{-\frac{2r}{\xi} + \left(\frac{r}{\xi}\right)^{1/3} \Gamma' + \left(\frac{r}{\xi}\right)^{2/3} \Gamma'' + \Lambda'}, \end{aligned} \quad (10)$$

where $\sigma[\ln |\psi(\mathbf{r})|^2] \sim r^{1/3}$, and new constants Γ' , Γ'' , and Λ' are introduced. Figure 4(b) compares this prediction with numerical data for $\langle |\psi(\mathbf{r})|^2 \rangle$. Notably, the values of Γ' , Γ'' , and Λ' are not fitted from $\langle |\psi(\mathbf{r})|^2 \rangle$, but instead determined from the typical wave packet and the GUE TW distribution $P_{\text{TW}}(\tilde{\chi})$.

The excellent agreement between Eqs. (9), (10) and the numerical data predicts a stretched exponential correction to the exponential decay of 2D localization; see SM [78] for more details. Notably, the absence of this stretched exponential correction in 1D Anderson localization, where Gaussian fluctuations of the logarithm of the wave density have zero average [20], underscores its distinctive signature in 2D localization.

Conclusion.—In this Letter, we have unveiled previously unknown and highly significant features of two-dimensional Anderson localization of wave packets through an analogy with KPZ physics. Notably, we have discovered that the

fluctuations of the logarithm of the wave density exhibit an algebraic growth with the KPZ growth exponent of $1/3$, providing a stretched exponential correction to the prevailing exponential localization behavior in two dimensions. Compared to the unrealistic conditions for experiments in solid-state devices, such as zero-temperature and non-interacting systems required for conductance fluctuations exhibiting KPZ physics [37–41], our findings have direct experimental accessibility with cold atom systems and classical waves [29,52,55,58,59,61–63,76,90], opening up exciting opportunities for experimental validation and further exploration. Moreover, our extensive numerical results demonstrate that the critical exponents and statistical distributions governing KPZ physics are universally present in localized wave packets in two dimensions. Indeed, while our computational results are based on a variant of the kicked rotor, we have confirmed the validity of our observations in the two-dimensional Anderson model (see SM [78]). We have omitted time effects from our description. In the regime of large times $t \gg t_{\text{loc}}$, the spatial distributions reach a stationary state, which implies that our findings are relevant for any fixed time $t \gg t_{\text{loc}}$. However, in addition to the spatial perspective, the wave packet observable also provides insight into the temporal fluctuations. This opens up intriguing possibilities for investigating the dynamical glassy properties inherent in the DP problem [91], including phenomena such as aging [92,93]. The integration of KPZ and directed polymer physics insights holds also great promise in shedding light on the as-yet-unclear aspects of Anderson localization in high dimensions [94–97].

G. L. expresses gratitude for enlightening discussions with the late D. Delande. We thank B. Georgeot, N. Izem, P. Le Doussal, C. Miniatura, M. Richard, and G. Schehr for fruitful discussions, and M. Richard for a careful reading of the manuscript. This study has been supported through the research funding Grants No. ANR-17-CE30-0024, No. ANR-18-CE30-0017, and No. ANR-19-CE30-0013, and by the Singapore Ministry of Education Academic Research Fund Tier I (WBS No. R-144-000-437-114). J. G. also acknowledges the support from the Singapore National Research Foundation via the Project No. NRF2021-QEP2-02-P09, as well as the support by the National Research Foundation, Singapore and A*STAR under its CQT Bridging Grant. The computational work for this Letter was performed on resources of the National Supercomputing Centre, Singapore and Calcul en Midi-Pyrénées (CALMIP), France.

*Corresponding author: senmu@u.nus.edu

†Corresponding author: phygj@nus.edu.sg

‡Corresponding author: lemarie@irsamc.ups-tlse.fr

[1] H. Fischer, *A History of the Central Limit Theorem: From Classical to Modern Probability Theory* (Springer, New York, 2011).

- [2] G. E. Uhlenbeck and L. S. Ornstein, *Phys. Rev.* **36**, 823 (1930).
 [3] M. C. Wang and G. E. Uhlenbeck, *Rev. Mod. Phys.* **17**, 323 (1945).
 [4] M. Kardar, G. Parisi, and Y.-C. Zhang, *Phys. Rev. Lett.* **56**, 889 (1986).
 [5] I. Corwin, *Random Matrices Theory Appl.* **01**, 1130001 (2012).
 [6] K. A. Takeuchi, *Physica (Amsterdam)* **504A**, 77 (2018).
 [7] H. Spohn, *J. Stat. Mech.* (2020) 044001.
 [8] T. Jin and D. G. Martin, *Phys. Rev. Lett.* **129**, 260603 (2022).
 [9] M. Ljubotina, M. Žnidarič, and T. Prosen, *Phys. Rev. Lett.* **122**, 210602 (2019).
 [10] A. Scheie, N. E. Sherman, M. Dupont, S. E. Nagler, M. B. Stone, G. E. Granroth, J. E. Moore, and D. A. Tennant, *Nat. Phys.* **17**, 726 (2021).
 [11] D. Wei, A. Rubio-Abadal, B. Ye, F. Machado, J. Kemp, K. Srakaew, S. Hollerith, J. Rui, S. Gopalakrishnan, N. Y. Yao, I. Bloch, and J. Zeiher, *Science* **376**, 716 (2022).
 [12] A. Nahum, J. Ruhman, S. Vijay, and J. Haah, *Phys. Rev. X* **7**, 031016 (2017).
 [13] Q. Fontaine, D. Squizzato, F. Baboux, I. Amelio, A. Lemaître, M. Morassi, I. Sagnes, L. Le Gratiet, A. Harouri, M. Wouters, I. Carusotto, A. Amo, M. Richard, A. Minguzzi, L. Canet, S. Ravets, and J. Bloch, *Nature (London)* **608**, 687 (2022).
 [14] P. W. Anderson, *Phys. Rev.* **109**, 1492 (1958).
 [15] E. Abrahams, P. W. Anderson, D. C. Licciardello, and T. V. Ramakrishnan, *Phys. Rev. Lett.* **42**, 673 (1979).
 [16] E. Abrahams, *50 Years of Anderson Localization* (World Scientific, Singapore, 2010).
 [17] P. A. Lee and A. D. Stone, *Phys. Rev. Lett.* **55**, 1622 (1985).
 [18] P. A. Mello, *Phys. Rev. Lett.* **60**, 1089 (1988).
 [19] C. W. J. Beenakker, *Rev. Mod. Phys.* **69**, 731 (1997).
 [20] A. D. Mirlin, *Phys. Rep.* **326**, 259 (2000).
 [21] P. A. Lee and T. V. Ramakrishnan, *Rev. Mod. Phys.* **57**, 287 (1985).
 [22] F. Evers and A. D. Mirlin, *Rev. Mod. Phys.* **80**, 1355 (2008).
 [23] F. Wegner, *Z. Phys. B Condens. Matter* **36**, 209 (1980).
 [24] C. Castellani and L. Peliti, *J. Phys. A* **19**, L429 (1986).
 [25] M. Feigel'man, L. Ioffe, V. Kravtsov, and E. Cuevas, *Ann. Phys. (Amsterdam)* **325**, 1390 (2010).
 [26] A. Gogolin, *Sov. Phys. JETP* **44**, 1003 (1976), <http://jetp.ras.ru/cgi-bin/e/index/e/44/5/p1003?a=list>.
 [27] A. Gogolin, V. I. Mel'nikov, and E. Rashba, *Sov. Phys. JETP* **42**, 168 (1975), <http://jetp.ras.ru/cgi-bin/e/index/e/42/1/p168?a=list>.
 [28] K. Efetov and A. Larkin, *Sov. Phys. JETP* **58**, 444 (1983), <http://jetp.ras.ru/cgi-bin/e/index/e/58/2/p444?a=list>.
 [29] C. Hainaut, J.-F. Clément, P. Szrftgiser, J. C. Garreau, A. Rançon, and R. Chicireanu, *Eur. Phys. J. D* **76**, 103 (2022).
 [30] E. A. Stern, *Phys. Rev. B* **7**, 1303 (1973).
 [31] V. Nguen, B. Spivak, and B. Shklovskii, *Sov. Phys. JETP* **62**, 1021 (1985), <http://jetp.ras.ru/cgi-bin/e/index/e/62/5/p1021?a=list>.
 [32] E. Medina and M. Kardar, *Phys. Rev. B* **46**, 9984 (1992).
 [33] F. Pietracaprina, V. Ros, and A. Scardicchio, *Phys. Rev. B* **93**, 054201 (2016).
 [34] M. Kardar and Y.-C. Zhang, *Phys. Rev. Lett.* **58**, 2087 (1987).
 [35] T. Halpin-Healy and Y.-C. Zhang, *Phys. Rep.* **254**, 215 (1995).

- [36] F. Comets, *Directed Polymers in Random Environments* (Springer, Cham, 2017).
- [37] J. Prior, A. M. Somoza, and M. Ortuño, *Phys. Rev. B* **72**, 024206 (2005).
- [38] A. M. Somoza, M. Ortuño, and J. Prior, *Phys. Rev. Lett.* **99**, 116602 (2007).
- [39] J. Prior, A. M. Somoza, and M. Ortuño, *Eur. Phys. J. B* **70**, 513 (2009).
- [40] A. M. Somoza, P. Le Doussal, and M. Ortuño, *Phys. Rev. B* **91**, 155413 (2015).
- [41] G. Lemarié, *Phys. Rev. Lett.* **122**, 030401 (2019).
- [42] V. Dobrosavljević, N. Trivedi, and J. M. Valles Jr, *Conductor Insulator Quantum Phase Transitions* (Oxford University Press, New York, 2012).
- [43] M. Pollak, M. Ortuño, and A. Frydman, *The Electron Glass* (Cambridge University Press, Cambridge, England, 2013).
- [44] J. H. Davies, P. A. Lee, and T. M. Rice, *Phys. Rev. Lett.* **49**, 758 (1982).
- [45] M. Pollak and B. Shklovskii, *Hopping Transport in Solids* (Elsevier, New York, 1991), Vol. 28.
- [46] A. Vaknin, Z. Ovadyahu, and M. Pollak, *Phys. Rev. Lett.* **84**, 3402 (2000).
- [47] A. M. Somoza, M. Ortuño, M. Caravaca, and M. Pollak, *Phys. Rev. Lett.* **101**, 056601 (2008).
- [48] F. Ladieu and J.-P. Bouchaud, *J. Phys. I (France)* **3**, 2311 (1993).
- [49] F. Ladieu, M. Sanquer, and J. P. Bouchaud, *Phys. Rev. B* **53**, 973 (1996).
- [50] S. c. v. Bogdanovich and D. Popović, *Phys. Rev. Lett.* **88**, 236401 (2002).
- [51] J. Jaroszyński and D. Popović, *Phys. Rev. Lett.* **99**, 046405 (2007).
- [52] F. L. Moore, J. C. Robinson, C. Bharucha, P. E. Williams, and M. G. Raizen, *Phys. Rev. Lett.* **73**, 2974 (1994).
- [53] F. L. Moore, J. C. Robinson, C. F. Bharucha, B. Sundaram, and M. G. Raizen, *Phys. Rev. Lett.* **75**, 4598 (1995).
- [54] G. Roati, C. D'Errico, L. Fallani, M. Fattori, C. Fort, M. Zaccanti, G. Modugno, M. Modugno, and M. Inguscio, *Nature (London)* **453**, 895 (2008).
- [55] J. Billy, V. Josse, Z. Zuo, A. Bernard, B. Hambrecht, P. Lugan, D. Clément, L. Sanchez-Palencia, P. Bouyer, and A. Aspect, *Nature (London)* **453**, 891 (2008).
- [56] A. Aspect and M. Inguscio, *Phys. Today* **62**, No. 8, 30 (2009).
- [57] L. Sanchez-Palencia and M. Lewenstein, *Nat. Phys.* **6**, 87 (2010).
- [58] T. Schwartz, G. Bartal, S. Fishman, and M. Segev, *Nature (London)* **446**, 52 (2007).
- [59] M. Segev, Y. Silberberg, and D. N. Christodoulides, *Nat. Photonics* **7**, 197 (2013).
- [60] J. D. Maynard, *Rev. Mod. Phys.* **73**, 401 (2001).
- [61] H. Hu, A. Strybulevych, J. H. Page, S. E. Skipetrov, and B. A. van Tiggelen, *Nat. Phys.* **4**, 945 (2008).
- [62] I. Manai, J.-F. Clément, R. Chicireanu, C. Hainaut, J. C. Garreau, P. Szriftgiser, and D. Delande, *Phys. Rev. Lett.* **115**, 240603 (2015).
- [63] J. Chabé, G. Lemarié, B. Grémaud, D. Delande, P. Szriftgiser, and J. C. Garreau, *Phys. Rev. Lett.* **101**, 255702 (2008).
- [64] M. Lopez, J.-F. Clément, P. Szriftgiser, J. C. Garreau, and D. Delande, *Phys. Rev. Lett.* **108**, 095701 (2012).
- [65] K. A. Takeuchi, M. Sano, T. Sasamoto, and H. Spohn, *Sci. Rep.* **1**, 34 (2011).
- [66] T. Sasamoto and H. Spohn, *Phys. Rev. Lett.* **104**, 230602 (2010).
- [67] P. Calabrese, P. Le Doussal, and A. Rosso, *Europhys. Lett.* **90**, 20002 (2010).
- [68] V. Dotsenko, *Europhys. Lett.* **90**, 20003 (2010).
- [69] P. Calabrese and P. Le Doussal, *Phys. Rev. Lett.* **106**, 250603 (2011).
- [70] A. K. Hartmann, A. Krajenbrink, and P. Le Doussal, *Phys. Rev. E* **101**, 012134 (2020).
- [71] G. Casati, B. V. Chirikov, F. M. Izraelev, and J. Ford, in *Stochastic Behavior in Classical and Quantum Hamiltonian Systems*, edited by G. Casati and J. Ford (Springer Berlin Heidelberg, Berlin, Heidelberg, 1979), pp. 334–352.
- [72] S. Fishman, D. R. Grempel, and R. E. Prange, *Phys. Rev. Lett.* **49**, 509 (1982).
- [73] D. R. Grempel, S. Fishman, and R. E. Prange, *Phys. Rev. Lett.* **49**, 833 (1982).
- [74] D. R. Grempel, R. E. Prange, and S. Fishman, *Phys. Rev. A* **29**, 1639 (1984).
- [75] E. Doron and S. Fishman, *Phys. Rev. Lett.* **60**, 867 (1988).
- [76] G. Lemarié, H. Lignier, D. Delande, P. Szriftgiser, and J. C. Garreau, *Phys. Rev. Lett.* **105**, 090601 (2010).
- [77] M. Santhanam, S. Paul, and J. B. Kannan, *Phys. Rep.* **956**, 1 (2022).
- [78] See Supplemental Materials at <http://link.aps.org/supplemental/10.1103/PhysRevLett.132.046301> for detailed information on the mapping to the directed polymer problem, determination of the localization time, stretched-exponential correction to the wave packet exponential localization, and additional numerical results for the Anderson model in two dimensions.
- [79] Y.-C. Zhang, *Phys. Rev. Lett.* **62**, 979 (1989).
- [80] Y.-C. Zhang, *Europhys. Lett.* **9**, 113 (1989).
- [81] E. Medina, M. Kardar, Y. Shafir, and X. R. Wang, *Phys. Rev. Lett.* **62**, 941 (1989).
- [82] M. P. Gelfand, *Physica (Amsterdam)* **177A**, 67 (1991).
- [83] T. Blum and Y. Y. Goldschmidt, *Nucl. Phys.* **B380**, 588 (1992).
- [84] S. Roux and A. Coniglio, *J. Phys. A* **27**, 5467 (1994).
- [85] A. Gangopadhyay, V. Galitski, and M. Müller, *Phys. Rev. Lett.* **111**, 026801 (2013).
- [86] D. S. Fisher and D. A. Huse, *Phys. Rev. B* **43**, 10728 (1991).
- [87] C. Monthus and T. Garel, *J. Phys. A* **45**, 095002 (2012).
- [88] M. Mézard, *J. Phys. (Les Ulis, Fr.)* **51**, 1831 (1990).
- [89] B. Derrida and H. Spohn, *J. Stat. Phys.* **51**, 817 (1988).
- [90] A. Lagendijk, B. Van Tiggelen, and D. S. Wiersma, *Phys. Today* **62**, No. 8, 24 (2009).
- [91] K. J. Wiese, *Rep. Prog. Phys.* **85**, 086502 (2022).
- [92] H. Yoshino, *J. Phys. A* **29**, 1421 (1996).
- [93] A. Barrat, *Phys. Rev. E* **55**, 5651 (1997).
- [94] J. Arenz and M. R. Zirnbauer, arXiv:2305.00243.
- [95] I. García-Mata, J. Martin, O. Giraud, B. Georgeot, R. Dubertrand, and G. Lemarié, *Phys. Rev. B* **106**, 214202 (2022).
- [96] C. Monthus and T. Garel, *Phys. Rev. E* **74**, 011101 (2006).
- [97] M. Baroni, G. G. Lorenzana, T. Rizzo, and M. Tarzia, arXiv:2304.10365.